

## Dual-frequency ferromagnetic resonance

Y. Guan<sup>a)</sup> and W. E. Bailey

Materials Science Program, Department of Applied Physics, Columbia University, New York, New York 10027

(Received 3 February 2006; accepted 22 April 2006; published online 30 May 2006)

We describe a new experimental technique to investigate coupling effects between different layers or modes in ferromagnetic resonance (FMR). Dual FMR frequencies are excited (2–8 GHz) simultaneously and detected selectively in a broadband rf circuit using lock-in amplifier detection at separate modulation frequencies. © 2006 American Institute of Physics. [DOI: 10.1063/1.2204907]

### INTRODUCTION

Ferromagnetic resonance (FMR) precession of ferromagnetic alloys and heterostructures is technologically important since it determines the gigahertz dynamics of spin electronic devices. Recently, novel long-ranged dynamic coupling mechanisms between layers in heterostructures, through the transient excitation of spin currents, have been observed experimentally.<sup>1</sup> Some of these processes could be elucidated if motions of individual layers can be excited independently, allowing the effects of higher amplitude motion at one layer to be characterized in the resonance at an opposite layer.

Experiments on driven FMR modes in ferromagnetic multilayers so far have typically focused on the situation with single drive excitation. Dual-drive excitations cannot be found in the literature except in a few studies of nonlinear interactions between magnetostatic waves in yttrium-iron-garnet films.<sup>2,3</sup> We have developed a dual-frequency FMR technique to study interactions between FMR modes. Through the adjustment of pumping power at mode 1 (excited at  $f_1$ ), we can examine effects on FMR line intensity, width, or shape at mode 2 (excited at  $f_2$ ).

In this article, we describe the apparatus for dual-frequency FMR measurements. FMR is excited at two frequencies using dual rf sources, combined at a power divider, and delivered to the ferromagnetic sample using a broadband coplanar waveguide (CPW). The response of individual FMR modes is detected by modulating each rf source at a separate low modulation frequency and locking in to these two frequencies with separate lock-in amplifiers. The technique is validated with a  $\text{Ni}_{81}\text{Fe}_{19}$  thin film sample, where dual-frequency FMR is proven to be selective of resonance frequency. With this technique, investigations have been made in a  $\text{Ni}_{81}\text{Fe}_{19}/\text{Cu}/\text{Co}_{93}\text{Zr}_7$  multilayer, where some influence of pumped  $\text{Ni}_{81}\text{Fe}_{19}$  precession on the  $\text{Co}_{93}\text{Zr}_7$  resonance may be seen.

### APPARATUS

The block diagram of the experimental setup of dual-frequency FMR is shown in Fig. 1, where broadband

(2–8 GHz) swept-field FMR is measured. Lock-in amplifier detection through frequency modulation is used in our FMR measurements. Apart from the dual-frequency capability, our measurements are similar to conventional FMR cavity measurements,<sup>4</sup> although network analyzers are often used instead of lock-in amplifier for phase-sensitive detection in conventional broadband FMR spectrometers.<sup>5</sup>

The microwave sources consist of two independently controllable frequency sweepers: rf source 1 and rf source 2. rf source 1 is a homebuilt, fixed-frequency source at 2.3 GHz ( $f_1$ ), variable in output from –50 to 22 dBm. We used a filtered amplified higher harmonic of a 88 MHz signal from a Wavetek 3000 signal with FM capability. rf source 2 is a Wiltron 6668B sweep generator operated in cw mode, with tunable frequency ( $f_2$ ) in the range of 0–40 GHz, variable output from –50 to 15 dBm, and FM capability. The dual microwave generators are used to generate dual rf signals ( $f_1, f_2$ ) simultaneously. The two independent rf sources modulated at separate frequencies ( $f_{\text{mod}}^1, f_{\text{mod}}^2$ ) are combined with an Anaren 42020 broadband power combiner/divider (2–8 GHz), which attenuates each input by 3 dB in transmission, and then delivered to the ferromagnetic thin film sample through a lithographic CPW with a 100  $\mu\text{m}$  center conductor width. The rf field delivery configuration here is similar to that used in pulsed inductive microwave magnetometer (PIMM) measurements,<sup>6</sup> substituting cw microwave sources for the pulse generator.

The thin film sample is placed film side down onto the top of the CPW, with a thin layer of photoresist spin coated onto the film to prevent it from shorting the CPW. The CPW, used to pump the thin film sample with combined microwave (2–8 GHz) excitations from two synthesized microwave generators, is constructed by standard lithographic techniques and placed inside a Fe core electromagnet. The electromagnet has a gap of  $\sim 2$  cm and a maximum field of  $\sim 1.0$  T at 40 A, controlled by parallel Kepco-BOP-20/20M current sources. The Fe core electromagnet provides applied magnetic bias field along the center conductor of CPW, which is measured directly using a transverse Hall probe monitored by a Lakeshore 421 gaussmeter.

Transmitted rf signals through the magnetic thin film sample are detected at a microwave diode (0–18 GHz), the output of which is sent to the A inputs of two lock-in ampli-

<sup>a)</sup>Electronic mail: yg2111@columbia.edu

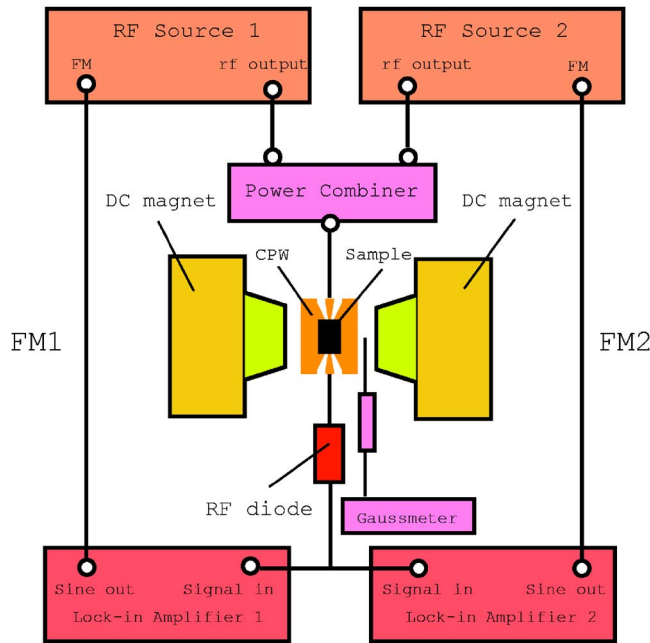


FIG. 1. (Color online) Block diagram of the experimental setup of dual-frequency FMR.

fiers (lock-in 1 of SR810 and lock-in 2 of SR830). The sine outputs of the lock-in amplifiers provide the modulation to the transmitted rf signals at separate modulation frequencies:  $f_{\text{mod}}^1$  ( $\sim 120$  Hz) for  $f_1$  and  $f_{\text{mod}}^2$  ( $\sim 540$  Hz) for  $f_2$ . A micro-computer equipped with a general purpose interface bus (GPIB) communicates with the SR810/830 and the Wiltron 6668B; analog inputs ( $\pm 10$  V) at the SR830 read the corrected output of the Lakeshore 421 gaussmeter, and parallel analog outputs ( $\pm 5$  V) control the Kepco power supplies. All these features allow the system to be fully automated.

In operation, the dual-frequency FMR measurement can sweep frequencies at  $f_2$  and fields  $H_B$ , while monitoring the diode signals at  $f_{\text{mod}}^1$  ( $f_1$ ) and  $f_{\text{mod}}^2$  ( $f_2$ ). Power levels at  $f_1$  are set manually through a variable attenuator. A high-precision Keithley 2000 digital multimeter (DMM), also under GPIB control, was available to monitor the dc diode signals in the same measurements.

## EXPERIMENT

A single layer sample of  $\text{Ni}_{81}\text{Fe}_{19}$  (25 nm) and a trilayer structure of  $\text{Ni}_{81}\text{Fe}_{19}$  (25 nm)/Cu (20 nm)/ $\text{Co}_{93}\text{Zr}_7$  (25 nm) were grown by UHV magnetron sputtering from alloy targets at a base pressure of  $4 \times 10^{-9}$  torr onto Si/SiO<sub>2</sub> substrates. A 20 Oe deposition field was applied to induce unidirectional anisotropy in the film plane. More details on deposition conditions can be found in our previous work.<sup>7</sup>

Conventional broadband FMR measurements (rf source 1 is off, and rf source 2 is on) were made on both  $\text{Ni}_{81}\text{Fe}_{19}$  and  $\text{Ni}_{81}\text{Fe}_{19}$ /Cu/ $\text{Co}_{93}\text{Zr}_7$  thin film samples at several selected frequencies (from 0 to 5 GHz) to determine the Kittel relations<sup>8</sup> between microwave frequency ( $\omega_p/2\pi$ ) and resonance field ( $H_{\text{res}}$ ). For in-plane magnetization in a thin film, the Kittel relation can be expressed as<sup>8</sup>

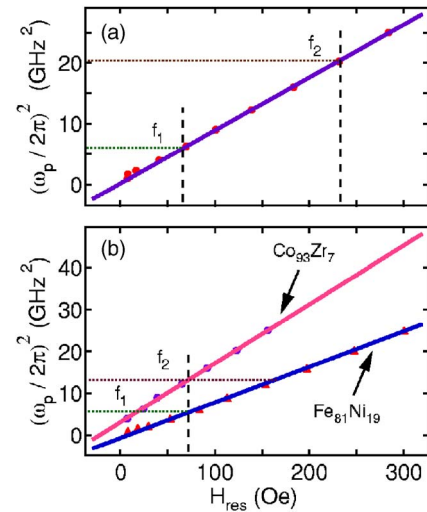


FIG. 2. (Color online) (a) Kittel plot of the single layer of  $\text{Ni}_{81}\text{Fe}_{19}$  thin film. (b) Kittel plot of the trilayer structure of  $\text{Ni}_{81}\text{Fe}_{19}/\text{Cu}/\text{Co}_{93}\text{Zr}_7$  thin film. Solid lines are linear fits.

$$\omega_p^2 \approx \mu_0^2 \gamma^2 M_s (H_{\text{res}} + H_k), \quad (1)$$

where  $H_k$  is an effective field due to anisotropy.

The  $\text{Ni}_{81}\text{Fe}_{19}$  thin film sample was then measured using dual-frequency FMR, where two different FMR modes were excited independently, using separate resonance frequencies ( $f_1=2.3$  GHz,  $f_2=4.5$  GHz) at a fixed field. In the  $\text{Ni}_{81}\text{Fe}_{19}/\text{Cu}/\text{Co}_{93}\text{Zr}_7$  trilayer sample, both the  $\text{Ni}_{81}\text{Fe}_{19}$  layer and the  $\text{Co}_{93}\text{Zr}_7$  layer were excited near resonance simultaneously, choosing  $H_{\text{res}}$  for  $f_1=2.3$  GHz, through the adjustment of  $f_2$  (to 3.8 GHz). The effects of variable power at  $f_1$  on the  $\text{Co}_{93}\text{Zr}_7$  resonance at  $f_2$  were investigated.

## RESULTS AND DISCUSSION

The results of conventional broadband FMR measurements on both  $\text{Ni}_{81}\text{Fe}_{19}$  and  $\text{Ni}_{81}\text{Fe}_{19}/\text{Cu}/\text{Co}_{93}\text{Zr}_7$  thin film samples are presented in Fig. 2. We show  $(\omega_p/2\pi)^2$  as a function of  $H_{\text{res}}$ .  $f_1$  and  $f_2$  denote the selected frequencies of excited FMR modes in dual-frequency FMR measurements on the same samples (shown in Figs. 3 and 4). Solid lines are linear fits based on Eq. (1). Two branches were observed for the  $\text{Ni}_{81}\text{Fe}_{19}/\text{Cu}/\text{Co}_{93}\text{Zr}_7$  thin film sample, corresponding

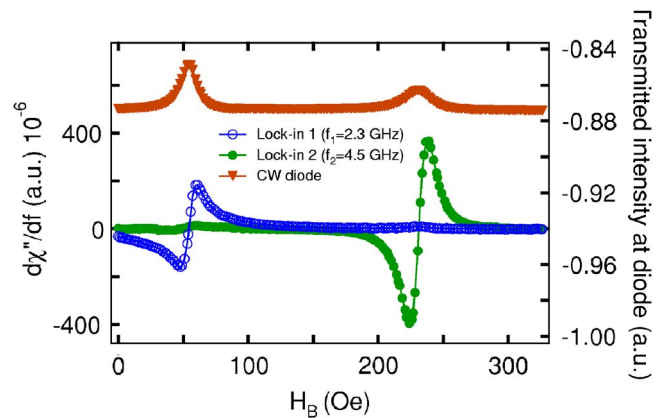


FIG. 3. (Color online) Dual-frequency FMR spectra ( $f_1=2.3$  GHz,  $f_2=4.5$  GHz) of  $\text{Ni}_{81}\text{Fe}_{19}$  thin film using dual lock-in detection.

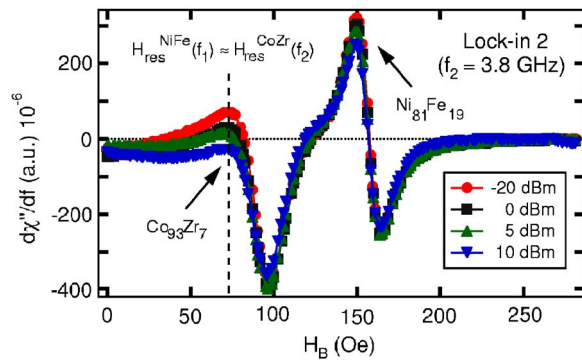


FIG. 4. (Color online) Dual-frequency FMR spectra at  $f_2=3.8$  GHz as a function of pumped power at  $f_1=2.3$  GHz in  $\text{Ni}_{81}\text{Fe}_{19}(25\text{ nm})/\text{Cu}(20\text{ nm})/\text{Co}_{93}\text{Zr}_7(25\text{ nm})$  thin film. The field  $H_B$  for simultaneous FMR of  $\text{Ni}_{81}\text{Fe}_{19}$  and  $\text{Co}_{93}\text{Zr}_7$  is indicated.

mostly to the separate resonances of the  $\text{Ni}_{81}\text{Fe}_{19}$  layer and the  $\text{Co}_{93}\text{Zr}_7$  layer, with some weak ferromagnetic coupling ( $\sim 5$  Oe).

Validation of frequency selectivity in dual-frequency FMR is shown in Fig. 3. Two different FMR modes were excited in the  $\text{Ni}_{81}\text{Fe}_{19}$  thin film sample at two selective resonance frequencies ( $f_1=2.3$  GHz,  $f_2=4.5$  GHz) and then detected selectively using dual lock-in amplifiers (lock-in 1, lock-in 2) respectively. Two absorption peaks were observed for the total transmitted signal, where the positions and widths of the two absorption peaks correspond closely with those found selectively at  $f_1$  and  $f_2$ .

Dual-frequency FMR measurement on the  $\text{Ni}_{81}\text{Fe}_{19}/\text{Cu}/\text{Co}_{93}\text{Zr}_7$  trilayer thin film sample is presented in Fig. 4, where the effects of pumped  $\text{Ni}_{81}\text{Fe}_{19}$  precession at  $f_1=2.3$  GHz were investigated on the  $\text{Co}_{93}\text{Zr}_7$  resonance at  $f_2=3.8$  GHz. This frequency ( $f_1$ ) sets the  $\text{Ni}_{81}\text{Fe}_{19}$  layer into FMR at  $H_B=72.5$  Oe. With rf power of rf source 2 fixed at a low value ( $-5$  dBm), we varied the pumping power of rf source 1, from  $-20$  to  $+10$  dBm, measured at the diode. As shown in Fig. 4, two separate FMR modes were observed for each value of the pumping power of rf source 1, where the mode at the low-field side corresponded primarily to the resonance of the  $\text{Co}_{93}\text{Zr}_7$  layer. Some variations can be seen in both the line intensity and the symmetry of the  $\text{Co}_{93}\text{Zr}_7$  FMR modes as a function of power pumped into the  $\text{Ni}_{81}\text{Fe}_{19}$  resonance. It is also evident that the high power excited at  $f_1$  has no discernible influence on the  $\text{Ni}_{81}\text{Fe}_{19}$  resonance measured at  $f_2$ , as expected. However, a quantitative estimate of

any dynamic coupling between  $\text{Ni}_{81}\text{Fe}_{19}$  and  $\text{Co}_{93}\text{Zr}_7$  layers could not be made as the residual influence of the static ( $\sim 5$  Oe) coupling could not be excluded. It is additionally important to drive the  $\text{Ni}_{81}\text{Fe}_{19}$  resonance symmetrically over the low-field region, which requires a second variable frequency source at  $f_1$ .

By using dual-frequency FMR technique, we can selectively excite several different FMR modes in a ferromagnetic alloy and heterostructures, and the nature of coupling interactions between multiple FMR modes could thus be probed. We remark that the technique presented could be extended to fixed-field, swept-frequency measurement, or to track the Kittel resonance at  $f_1$  as field  $H_{\text{res}}$  is swept. With much higher power amplification and some cooling capability, nonlinear interactions between magnetostatic spin-wave (MSSW) modes could be studied as well. Finally, the frequency range can be extended to 20 GHz, or even to 40 GHz, through the use of different power dividers.

In conclusion, a new experimental technique, dual-frequency ferromagnetic resonance (FMR), has been developed to investigate coupling effects between different FMR modes. This new technique is able to excite different FMR modes simultaneously and independently, while separating the properties of each.

## ACKNOWLEDGMENTS

This work was partially supported by the Army Research Office with Grant No. ARO-43986-MS-YIP, and the National Science Foundation with Grant No. NSF-DMR-02-39724. This work has used the shared experimental facilities that are supported primarily by the MRSEC(Columbia) program of the National Science Foundation under Contract No. NSF-DMR-0213574.

- <sup>1</sup>Y. Tserkovnyak, A. Brataas, G. E. W. Bauer, and B. I. Halperin, *Rev. Mod. Phys.* **77**, 1375 (2005).
- <sup>2</sup>D. J. Mar, T. L. Carroll, L. M. Pecora, J. F. Heagy, and F. J. Rachford, *J. Appl. Phys.* **80**, 1878 (1996).
- <sup>3</sup>D. J. Mar, T. L. Carroll, L. M. Pecora, and F. J. Rachford, *J. Appl. Phys.* **81**, 5734 (1997).
- <sup>4</sup>B. Heinrich, *Ultrathin Magnetic Structures II*, edited by B. Heinrich and J. A. C. Bland (Springer-Verlag, Berlin, 1994).
- <sup>5</sup>V. P. Denysenkov and A. M. Grishin, *Rev. Sci. Instrum.* **74**, 3400 (2003).
- <sup>6</sup>A. Kos, T. Silva, and P. Kabos, *Rev. Sci. Instrum.* **73**, 3563 (2002).
- <sup>7</sup>Y. Guan, Z. Dios, D. A. Arena, L. Cheng, and W. E. Bailey, *J. Appl. Phys.* **97**, 10A719 (2005).
- <sup>8</sup>C. Kittel, *Introduction to Solid State Physics* (Wiley, New York, 2005).